Impact of Maxwell rigidity transitions on resistance drift phenomena in GexTe12x glasses

Jennifer Luckas, A. Olk, P. Jost, H. Volkert, J. Alvarez, Alexandre Jaffré, Peter Zalden, Andrea Piarristeguy, Annie Pradel, Christophe Longeaud, et al.

AIP | Applied Physics Letters

Impact of Maxwell rigidity transitions on resistance drift phenomena in GexTe1x glasses

J. Luckas, A. Olk, P. Jost, H. Volker, J. Alvarez, A. Jaffré, P. Zalden, A. Piarristeguy, A. Pradel, C. Longeaud, and M. Wuttig

Citation: Applied Physics Letters **105**, 092108 (2014); doi: 10.1063/1.4893743
View online: http://dx.doi.org/10.1063/1.4893743
View Table of Contents: http://scitation.aip.org/content/aip/journal/apl/105/9?ver=pdfcov
Published by the AIP Publishing

Impact of Maxwell rigidity transitions on resistance drift phenomena in Ge_xTe_{1-x} glasses

J. Luckas,[1,2] A. Olk,[1,2] P. Jost,[1] H. Volker,[1] J. Alvarez,[2] A. Jaffré,[2] P. Zalden,[1] A. Piarristeguy,[3] A. Pradel,[3] C. Longeaud,[2] and M. Wuttig[1,4]
[1]*I.Physikalisches Institut, RWTH Aachen University, 52056 Aachen, Germany*
[2]*Laboratoire de Génie Electrique de Paris (CNRS UMR 8507), Supelec, Universités Paris VI et XI, Plateau de Moulon, 11 rue Joliot Curie, 91190 Gif sur Yvette, France*
[3]*Institut Charles Gerhardt Montpellier, UMR CNRS 5253, Université Montpellier 2, CC1503, 34095 Montpellier Cedex 5, France*
[4]*JARA Fundamentals of Future Information Technology, RWTH Aachen University, Germany*

(Received 1 June 2014; accepted 11 August 2014; published online 5 September 2014)

Amorphous chalcogenides usually exhibit a resistivity, which increases with age following a power law $\rho \sim t^{\alpha}$. Existing theories link this change in amorphous state resistivity to structural relaxation. Here, the impact of fundamental glass properties on resistance drift phenomena in amorphous Ge_xTe_{1-x} networks is studied. Employing Raman spectroscopy, the Maxwell rigidity transition from flexible to stressed rigid is determined to occur in the compositional range $0.250 < x_c < 0.265$. Stressed rigid glasses ($x > 0.265$) exhibit rather strong resistance drift, where the drift parameters increase steadily from $\alpha = 0.13$ for amorphous GeTe to $\alpha = 0.29$ for compositions near the stiffness threshold x_c. On the other hand, the drift parameter in flexible glasses ($x < 0.25$) decreases with decreasing Ge content x to values as low as $\alpha = 0.05$. These findings illustrate the strong impact of the stiffness threshold on resistance drift phenomena in chalcogenides. © *2014 AIP Publishing LLC*. [http://dx.doi.org/10.1063/1.4893743]

Amorphous Ge_xTe_{1-x} alloys have attracted considerable attention in recent decades due to a portfolio of unique properties.[1–4] Ge poor compositions, such as $Ge_{0.15}Te_{0.85}$, are good glass formers, and hence possess crystallization times of more than 100 μs.[5] In contrast crystallization times down to 1 ns have been verified for the phase change alloy GeTe.[6] This extraordinary combination of fast crystallization kinetics with a rather high crystallization temperature ($T_c \sim 180\,^{\circ}C$ (Refs. 5 and 7)) qualifies GeTe as a suitable material for information storage. Generally, information is encrypted in binary codes—in phase-change memory devices as high resistive amorphous and low resistive crystalline bits. Storage densities could be drastically increased if phase-change materials would offer the possibility to realize multi-level cells. In this concept, the cell resistance could be systematically altered by changing its amorphized volume. This requires, however, a stable amorphous state, i.e., a material with a time-independent resistance. Unfortunately, the amorphous state resistivity in amorphous GeTe as well as $Ge_{0.15}Te_{0.85}$ is observed to increase with increasing sample age. This effect, which is commonly denoted as resistance drift, may cause severe data corruption over time and thus hampers the realization of multi-level phase change memories. The change in electrical properties is generally attributed to the structural relaxation of the glassy state. In this work resistance drift phenomena in a-Ge_xTe_{1-x} systems are linked to fundamental glass properties. The rigidity theory first proposed by Phillips[8] classifies amorphous networks into flexible or rigid glasses. In this concept, strong covalent forces are expected to act as mechanical Lagrangian constraints defining the local atomic structure of the disordered solid. Covalent solids demonstrate two different types of bonding constraints. The Bond-stretching constraints n_α specify the distance between neighbouring atoms, whereas the bond bending constraints n_β define the bonding angle. In flexible glasses, the total number of internal constraints $n = n_\alpha + n_\beta$ is lower than the degrees of freedom per atom, i.e., $n < 3$ in three dimensional systems. In contrast, rigid glasses are over coordinated having a total number of Lagrangian constraints $n > 3$ per atom. Hence, flexible glasses allow local deformations, whereas deformations in stressed rigid glasses are blocked by bond connectivity. In 1983, Thorpe claimed that flexible glasses in the absence of weaker long range forces show zero-frequency normal vibrational modes, so called *floppy modes* which vanish at the stiffness threshold.[9] Generally, the coordination number r determines the number of bond-bending and bond stretching constraints to $n_\alpha = r/2$ and $n_\beta = 2r - 3$, respectively. However, in a recent work Micoulaut *et al.* have shown that in amorphous chalcogenides containing heavier elements, such as Te, not all bonding constraints are intact.[10] This study based on first-principle molecular-dynamics simulations verified $n_\beta \sim 3$ bonding constraints, instead of $n_\beta = 2 \times 4 - 3 = 5$ expected using the general Maxwell counting procedure for Ge atoms in amorphous Ge-Sb-Te networks. Furthermore, Micoulaut *et al.* classified a-GeTe to belong to the stressed rigid glasses, while a-$Ge_{0.15}Te_{0.85}$ was shown to be a flexible glass. This implies that a stiffness threshold x_c exists in the range $0.15 < x_c < 0.50$. Unfortunately, MD simulations exist only for a-$Ge_{0.15}Te_{0.85}$ and a-GeTe. However, the work of Micoulaut *et al.* indicates that a-$Ge_{0.15}Te_{0.85}$ lies closer to the Maxwell rigidity threshold x_c than a-GeTe. This is why, we estimate the critical Ge concentration x_c using the coordination numbers and bond bonding constraints reported for the flexible a-$Ge_{0.15}Te_{0.85}$ composition (a-$Ge_{0.15}Te_{0.85}$: $r_{Ge} = 4.0$, $r_{Te} = 2.6$, $n_\beta^{Ge} = 3.3$, and $n_\beta^{Te} = 1.0$),[10] see the following equation:

$$n_C = x_c \cdot \frac{r_{Ge}}{2} + (1 - x_c)\frac{r_{Te}}{2} + x_c \cdot n_\beta^{Ge} + (1 - x_c) n_\beta^{Te} \equiv 3$$
$$\Rightarrow x_c \sim 0.23. \quad (1)$$

Literature reports drastic changes in thermal, structural, vibrational and electronic properties at the stiffness threshold in chalcogenide glasses.[11] The aim of this work is to investigate the impact of the Maxwell rigidity transition on resistance drift phenomena in Ge_xTe_{1-x} glasses. Thin a-Ge_xTe_{1-x} films with different Ge contents x have been produced by dc magnetron sputtering ($x = 0.15$ and $x = 0.50$; film thickness 200 nm) or dc magnetron co-sputtering ($0.15 < x < 0.50$; film thickness 80 nm) using a LS 320 von Ardenne system at a background pressure of 10^{-6} mbar and a Ar sputtering gas pressure of 5×10^{-3} mbar. Thin GeTe and $Ge_{0.15}Te_{0.85}$ have been deposited from one stoichiometric target using a sputtering power of 20 W. Within the co-sputtering deposition process, the sputtering power of the stoichiometric GeTe target has been fixed to 25 W, whereas the sputtering power at the stoichiometric $Ge_{0.15}Te_{0.85}$ target has been varied systematically between 10 and 70 W. Ge concentration x, film thickness d and optical properties such as the optical band gap E_G^α have been studied by a combination of Rutherford Backscattering (RBS), Energy Dispersive X-Ray spectroscopy (EDX), and ellipsometry measurements, where all methods give consistent results. Indeed, Eq. (1) serves as a rough estimate for the stiffness threshold in Ge_xTe_{1-x} glasses, only. Hence, the rigidity transition requires further experimental validation. Raman spectroscopy has been qualified as an excellent tool to identify the Maxwell rigidity transition in a-Ge_xS_{1-x} and a-Ge_xSe_{1-x} systems.[11,12] Fig. 1 shows Raman spectra taken on a-Ge_xTe_{1-x} thin films for different Ge concentrations x deposited on silicon substrates. These Raman spectra have been measured by a Confocal WITec alpha 300 Raman Microscope equipped with a WITec UHTS 300 spectrometer. The exciting laser source (532 nm) has been adjusted to a laser power of 34 μW at a beam diameter of 1 μm to prevent crystallization of the amorphous thin films studied. The actual temperature profile within the sample was determined using COMSOL Multiphysics. These simulations show that a continuous illumination of the sample surface with a power density of 34 $\mu W/cm^2$ increases the sample temperature to maximal 50 °C, which lies significantly below the crystallization temperature of Ge_xTe_{1-x} glasses.[5] A good signal to noise ratio could be achieved using a spectrometer grating of 1800 lines/mm and 30 accumulations of 20 s integration time. As reported in previous studies a-GeTe demonstrates four main modes at $\nu \sim 83\,cm^{-1}$, $\nu \sim 122\,cm^{-1}$, $\nu \sim 162\,cm^{-1}$, and $\nu \sim 220\,cm^{-1}$.[13] According to Mazzarello *et al.* vibrations in defective octahedral environments denoted in the following as $dOCTA^1$ and $dOCTA^2$ result in Raman modes at $\nu \sim 122\,cm^{-1}$ ($dOCTA^1$) and $\nu \sim 162\,cm^{-1}$ ($dOCTA^2$). Furthermore, Mazzarello *et al.* claim that the Raman modes above $220\,cm^{-1}$ originate from bond stretching of tetrahedral bonded Ge-Ge, whereas Raman peaks below $100\,cm^{-1}$ are mostly due to three fold coordinated tellurium.[14] Consequently, we refer to the lowest main peak at $\nu \sim 83\,cm^{-1}$ as the $3_{fold}Te$ Raman mode. Except a strong increase in relative intensity of the $dOCTA^1$ mode, no drastic changes in the Raman spectra are observed decreasing the Ge concentration from $x = 0.500$ to $x = 0.265$, see Fig. 1 and Table I. This strong increase with decreasing Ge content suggests that the $dOCTA^1$ mode is related to bonding arrangements involving Te. All Te rich compositions characterized by $x < 0.25$ demonstrate an additional peak at $\nu \sim 140\,cm^{-1}$, see Fig. 1 and Tables I and II. The presence of a floppy mode in amorphous Ge_xTe_{1-x} networks allows to determine the stiffness threshold to lie within the range $0.250 < x_c < 0.265$ Consequently, the stiffness threshold x_c is found to lie slightly higher than expected from the theoretical approximation using Eq. (1). Raman modes at $\nu \sim 140\,cm^{-1}$ and $\nu \sim 122\,cm^{-1}$ have been observed in a-Te as well.[15] Hence, this feature is probably linked to vibrations in Te bonds. Furthermore, chalcogenide glasses may demonstrate nanoscale phase separation with decreasing chalcogen content. The glass transition temperature is a measure for bond connectivity and exhibits a pronounced maximum at the composition, where nanoscale phase separation starts to form.[16] In contrast to Ge_xSe_{1-x} glasses,[16] the glass transition temperature in amorphous Ge_xTe_{1-x} systems is found to increase steadily by increasing the Ge content from x = 0.10 to x = 0.33.[17,18] Consequently, we conclude the absence of nanoscale phase separation in this regime. Due to

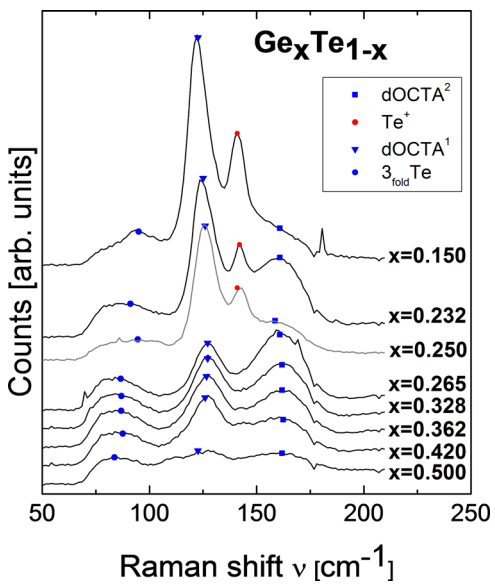

FIG. 1. Raman spectra taken on a-Ge_xTe_{1-x} glasses reveal significant changes upon passing the stiffness threshold x_c. Ge concentrations above $x \geq 0.265$ are characterized by distinct Raman modes at $\nu \sim 85\,cm^{-1}$ ($3_{fold}Te$), $\nu \sim 125\,cm^{-1}$ ($dOCTA^1$) and $\nu \sim 160\,cm^{-1}$ ($dOCTA^2$). Below the threshold $x \leq 0.250$, an additional Raman mode appears at $\nu \sim 140\,cm^{-1}$(Te^+). This finding indicates a Maxwell rigidity transition with decreasing Ge content as verified for Ge_xSe_{1-x} and Ge_xS_{1-x} glasses in previous studies. In amorphous Ge_xTe_{1-x} networks, the Maxwell rigidity transition lies within the compositional range $0.250 < x_c < 0.265$.

TABLE I. Fit results describing the Raman spectra taken on rigid Ge_xTe_{1-x} glasses.

Ge content x		0.500	0.420	0.362	0.328	0.265
$3_{fold}Te$	I_{rel}	0.83	0.58	0.57	0.54	0.43
	ν (cm^{-1})	***83.3***	***87.6***	***86.9***	***87.0***	***86.7***
$dOCTA^1$	I_{rel}	1.00	1.00	1.00	1.00	0.80
	ν (cm^{-1})	***122.3***	***126.0***	***126.6***	***127.2***	***127.2***
$dOCTA^2$	I_{rel}	0.64	0.74	0.82	0.95	1.00
	ν (cm^{-1})	***162.2***	***158.2***	***160.5***	***160.6***	***160.2***

TABLE II. Fit results describing the Raman spectra taken on flexible Ge_xTe_{1-x} glasses.

Ge content x		0.250	0.246	0.226	0.206	0.167	0.150
3_{fold}Te	I_{rel}	0.14	0.19	0.13	0.14	0.13	0.15
	ν (cm^{-1})	***94.57***	***92.25***	***95.79***	***93.93***	***89.79***	***95.0***
dOCTA[1]	I_{rel}	1.00	1.00	1.00	1.00	1.00	1.00
	ν (cm^{-1})	***125.96***	***125.98***	***125.85***	***125.5***	***124.07***	***122.7***
dOCTA[2]	I_{rel}	0.26	0.43	0.26	0.42	0.36	0.15
	ν (cm^{-1})	***158.7***	***159.0***	***157.64***	***157.27***	***143.53***	***160.0***
Te^+	I_{rel}	0.41	0.38	0.40	0.37	0.28	0.51
	ν (cm^{-1})	***141.45***	***141.48***	***141.60***	***141.04***	***141.13***	***140.3***

the observed drastic changes in the measured Raman and the absence of nano phase separation—the Maxwell rigidity transition is verified to occur within the compositional range $0.25 < x_c < 0.265$. Consequently, we identify Ge_xTe_{1-x} networks with Ge concentration $x > 0.265$ as rigid and $x < 0.25$ as floppy glasses.

In chalcogenides, an increase of the amorphous state resistivity after laser amorphization is usually observed to follow a power law of the form[19–22]

$$\rho(t) = \rho_0 \left(\frac{t}{t_0}\right)^{\alpha}. \tag{2}$$

Here, the parameter ρ_0 denotes the resistivity at time t_0, i.e., $\rho(t_0) = \rho_0$. Furthermore, the drift parameter α determines the change in resistivity: The higher the value of α, the stronger the resistance drift. In amorphous deposited films, the drift of the amorphous state resistivity should be expected to occur during or at least directly after the deposition process. Hence, a significant time span between sample fabrication and start of the drift measurement can be minimized but not avoided. Consequently, the evolution of the amorphous state resistivity in amorphous deposited chalcogenides demonstrates a shifted time scale[7,23]

$$\rho(t) = \rho_0 \left(\frac{t - t'}{t_0}\right)^{\alpha}. \tag{3}$$

Please note here, that resistance drift phenomena observed in laser amorphized material can be measured directly after vitrification, which leads to $t' = 0$.

To study the impact of Maxwell's rigidity transition on resistance drift phenomena the change in amorphous state resistivity has been measured by annealing at 50 °C over 24 or 48 h, respectively. Furthermore, all drift measurements have been performed in a protective atmosphere to avoid oxidation. Table III lists the drift parameters obtained for all chalcogenide thin films studied. A comparison of drift parameters α versus Ge concentration x reveals the strong impact of the Maxwell transition, see Fig. 2. In floppy glasses, the drift parameter α decreases steadily with decreasing Ge content x to values as low as $\alpha = 0.05$. In contrast compositions classified as stressed rigid show high drift coefficients, i.e., $\alpha > 0.1$. Furthermore, the drift parameter α increases with decreasing Ge concentration x down to $\alpha = 0.29$ for compositions near the stiffness threshold. Obviously the stiffness threshold x_c has a strong impact on resistance drift. Previous works on amorphous stressed-rigid phase-change materials[22,24] report a high drift parameter α for alloys showing high activation energies E_A, which describes the thermal activation of the amorphous state resistivity according to

$$\rho(T) = \rho^* \cdot \exp\left(\frac{E_A}{k_b T}\right). \tag{4}$$

Table III displays activation energies measured during the heat up of the drift experiment at 50 °C compared to optical band gap values determined as described in Ref. 24. The activation energies as well as the optical band gap are observed to increase by decreasing the Ge concentration from $x = 0.50$ to $x = 0.265$. In stressed rigid glasses, the drift parameter α is thus related to the activation energy E_A: low drifting materials are characterized by low and strong drifting materials by a high activation energy E_A (see the last five columns of Table III). Obviously, floppy Ge_xTe_{1-x} glasses do not follow this rule of thumb, and thus show a general different resistance drift behaviour as compared with the stressed-rigid phase-change alloys. The different drift behaviour probably originates from fundamental differences in the density of states within the forbidden energy band gap, which can be investigated by Modulated Photocurrent Experiments. Whereas strongly drifting phase-change materials such as a-GeTe or a-$Ge_2Sb_2Te_5$ demonstrate distinct peaked defect distributions around 0.2 eV from the valence band edge as well as deep states near mid gap, the flexible alloy $Ge_{0.15}Te_{0.85}$ does not show any peaked defect distributions.[25] Hence, Modulated Photocurrent Experiments on a-$Ge_{0.15}Te_{0.85}$ observe valence band tail states only. We repeated similar experiments for the floppy a-$Ge_{0.25}Te_{0.75}$

TABLE III. Optical band gaps E_g^x, activation energies of electronic conduction E_A, and drift parameters α defined in Eq. (3).

Ge content	0.150	0.167	0.206	0.226	0.246	0.250	0.265	0.328	0.362	0.420	0.500
α	0.05	0.07	0.09	0.11	0.13	0.17	0.28	0.29	0.28	0.18	0.13
E_A (eV)	0.43	0.46	0.48	0.48	0.48	0.47	0.46	0.43	0.41	0.37	0.36
E_g^x (eV)	0.973	1.028	1.047	1.039	1.031	1.016	0.959	0.925	0.905	0.841	0.762

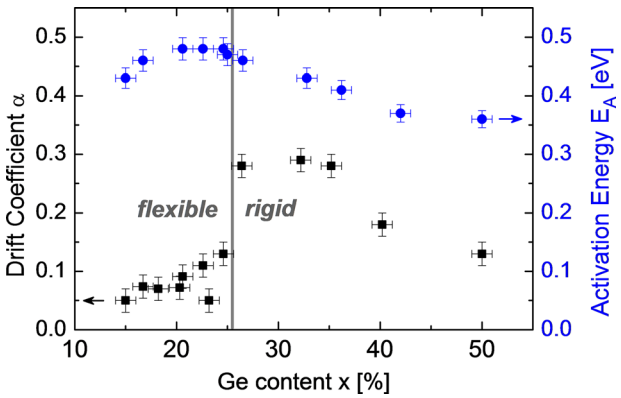

FIG. 2. Activation energies E_A (blue dots) and drift parameters α (black squares) measured at the beginning of the drift experiment at 50 °C over 24 h in amorphous Ge_xTe_{1-x} thin films with different Ge concentration x. All stressed rigid glasses demonstrate high values for α ranging from $\alpha = 0.13$ for a-GeTe up to $\alpha \sim 0.29$ for compositions near the stiffness threshold marked by the vertical bar. On the contrary, the drift coefficient tends to decrease with decreasing Ge content x in flexible glasses. Therefore, the Maxwell rigidity transition has a pronounced impact on resistance drift phenomena in Ge_xTe_{1-x} glasses.

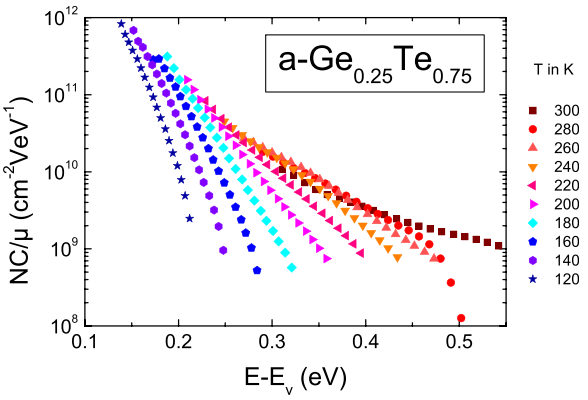

FIG. 3. Reduced density of states Nc/μ measured by Modulated Photocurrent Experiments on a-$Ge_{0.25}Te_{0.75}$. A detailed discussion on the method applied to amorphous chalcogenides can be found in Refs. 7, 24, and 25. The common envelope of the curves each taken at a different temperature reveals the density of states from the valence band edge E_v towards mid-gap. Apparently, the flexible compound a-$Ge_{0.25}Te_{0.75}$ does not demonstrate any peaked defect distribution. In the temperature range from 120 K to 300 K only valence band tail states are detected.

alloy. The results are shown in Figure 3. As for a-$Ge_{0.15}Te_{0.85}$, the floppy $Ge_{0.25}Te_{0.75}$ glass does show valence band tail states, but no peaked defect distributions, which arise from structural defects. Probably a flexible network hampers the creation of structural defects, whose evolution over time are shown to be responsible for the strong increase of the amorphous state resistivity in the phase change alloy a-GeTe.[25]

The rigidity transition in a-Ge_xTe_{1-x} glasses has been verified by means of Raman spectroscopy and falls into the compositional range $0.250 < x_c < 0.265$. The stiffness threshold is shown to have a large impact on resistance drift phenomena in a-Ge_xTe_{1-x} systems. In flexible glasses classified by the condition $x < x_c$, the drift parameter decreases with decreasing Ge content x to values as low as $\alpha = 0.05$. In contrast, stressed rigid glasses with $x > x_c$ show high drift coefficients $\alpha > 0.1$. In these stressed rigid glasses, the drift parameter α increases towards the stiffness threshold, which originates from an increase in activation energy E_A as observed for amorphous phase-change alloys in previous studies.

We acknowledge funding by the DFG (German Science Foundation) within the collaborative research centre SFB 917 "Nanoswitches." Furthermore, we would like to thank Dr. Alex Redinger from the University of Luxembourg for the performance and analysis of the EDX data presented and Dr. Bernhard Holländer from the Peter Grünberg Institute for his support regarding the shown RBS measurements.

[1]A. Zakery and S. R. Elliott, J. Non-Cryst. Solids **330**, 1–12 (2003).
[2]K. Tanaka, Phys. Rev. B **39**, 1270–1279 (1989).
[3]S. R. Ovshinsky, Phys. Rev. Lett. **21**, 1450–1453 (1968).
[4]M. Wuttig and N. Yamada, Nat. Mater. **6**, 824 (2007).
[5]M. Chen, K. A. Rubin, and R. W. Barton, Appl. Phys. Lett. **49**, 502–504 (1986).
[6]G. Bruns, P. Merkelbach, C. Schlockermann, M. Salinga, M. Wuttig, T. D. Happ, J. B. Philipp, and M. Kund, Appl. Phys. Lett. **95**, 043108 (2009).
[7]J. Luckas, A. Piarristeguy, G. Bruns, P. Jost, S. Grothe, R. M. Schmidt, C. Longeaud, and M. Wuttig, J. Appl. Phys. **113**, 023704 (2013).
[8]J. C. Phillips, J. Non-Cryst. Solids **34**, 153 (1979).
[9]M. F. Thorpe, J. Non-Cryst. Solids **57**, 355 (1983).
[10]M. Micoulaut, J.-Y. Raty, C. Otjacques, and C. Bichara, Phys. Rev. B **81**, 174206 (2010).
[11]X. Feng, W. Bresser, and P. Boolchand, Phys. Rev. Lett. **78**, 4422 (1997).
[12]M. Micoulaut and J. C. Phillips, J. Non-Cryst. Solids **353**, 1732 (2007).
[13]K. S. Andrikopoulos, S. N. Yannopoulos, G. A. Voyiatzis, A. V. Kolobov, M. Ribes, and J. Tominaga, J. Phys. Condens. Matter **18**, 965–979 (2006).
[14]R. Mazzarello, S. Caravati, S. Angioletti-Uberti, M. Bernasconi, and M. Parrinell, Phys. Rev. Lett. **104**, 085503 (2010).
[15]A. S. Pine and G. Dresselhaus, Phys. Rev. B **4**, 356 (1971).
[16]P. Boolchand, D. G. Georgiev, T. Qu, F. Wang, L. Cai, and S. Chakravarty, C. R. Chimie **5**, 713 (2002).
[17]P. Jóvári, A. A. Piarristeguy, R. Escalier, I. Kaban, J. Bednarcik, and A. Pradel, J. Phys.: Condens. Matter **25**, 195401–195409 (2013).
[18]J. P. DeNeufville, J. Non-Cryst. Solids **8–10**, 85–105 (1972).
[19]D. Ielmini, D. Sharma, S. Lavizzari, and A. L. Lacaita, IEEE Trans. Electron Devices **56**, 1070 (2009).
[20]I. V. Karpov, M. Mitra, D. Kau, G. Spadini, Y. A. Kryukov, and V. G. Karpov, J. Appl. Phys. **102**, 124503 (2007).
[21]A. Pirovano, A. L. Lacaita, F. Pellizzer, S. A. Kostylev, A. Benvenuti, and R. Bez, IEEE Trans. Electron Devices **51**, 714 (2004).
[22]M. Boniardi, A. Redaelli, A. Pirovano, I. Tortorelli, and F. Pellizzer, J. Appl. Phys. **105**, 084506 (2009).
[23]D. Krebs, R. M. Schmidt, J. Klomfaß, J. Luckas, G. Bruns, C. Schlockermann, M. Salinga, R. Carius, and M. Wuttig, J. Non-Cryst. Solids **358**, 2412–2415 (2012).
[24]J. Luckas, S. Kremers, D. Krebs, M. Salinga, M. Wuttig, and C. Longeaud, J. Appl. Phys. **110**, 013719 (2011).
[25]J. Luckas, D. Krebs, S. Grothe, J. Klomfaß, R. Carius, C. Longeaud, and M. Wuttig, J. Mater. Res. **28**, 1139 (2013).